Hydrogeological Investigation for the Assessment of Spring Pollution Due to Abandoned Mines in a Karst Area

Hujun Ren [1,2], Wanghua Sui [1,3,*], Xiangdong Meng [1,3] and Rui Guo [1,3]

[1] School of Resources and Geosciences, China University of Mining and Technology, Xuzhou 221116, China; LB13010027@cumt.edu.cn (H.R.); mengxiangdong123@cumt.edu.cn (X.M.); 05171798@cumt.edu.cn (R.G.)

[2] China Coal Hydrogeological Bureau Group Company, 18 Dafeng Road, Hongqiao District, Tianjin 300131, China

[3] Institute of Mine Water Hazards Prevention and Controlling Technology, China University of Mining and Technology, Xuzhou 221116, China

* Correspondence: suiwanghua@cumt.edu.cn; Tel.: +86-516-8359-1001

Abstract: This paper presents a hydrogeological investigation case study for assessing the sources and pathways of spring pollution in a karst area in Guizhou Province, Southern China. Our methods included hydrogeological surveys, geophysical surveys, cave detection, tracer tests, and borehole drilling. The results showed that the pollution of the Longdong Spring is controlled by the amount of rainfall, which also determines the duration of pollution. The concentration of Fe and Mn ions in the spring was found to exceed that in the code for drinking water quality (China) by more than 300 times. The investigations showed that the source of the pollution is the mine water drainage from the abandoned Feilong coal mine, which is located to the northwest of the Longdong Spring. The drainage to the spring was found to occur 24 h after the groundwater level in the goaf reached approximately +908 m above sea level. This indicates a recharge pathway between the abandoned mine and the Longdong Spring. Recommendations for grouting around the spring and sinkhole for pollution control are put forth.

Keywords: spring pollution; karst; tracer test; cave detection; geophysical survey; hydrogeological survey

1. Introduction

Karst is widely distributed in China, with a total area of approximately 3440×10^3 km^2, which accounts for about one third of the land area [1]. The exposed karst with an area of about 907×10^3 km^2 is mainly concentrated in Southwest China. Karst aquifers are composed of soluble rocks, often with large pathways and caves, which can store and transport a large amount of groundwater due to their strong permeability. Therefore, karst has a large potential for providing fresh water [2,3]. Karst areas generally develop in Southwest China due to its rich rainfall. Spring water is one of the most important water sources and its quantity and quality are always as good as the discharge of underground water. However, the spring water quality is vulnerable to pollution due to the complexity of karst aquifers [4].

In recent years, many coal mines have been abandoned in karst areas in China, and groundwater in the goaves has merged in the underground water system. The water in the goaves always contains high concentrations of Fe, Mn, and sulfate, with a high hardness and a low pH value, thus causing the pollution of spring water [5]. The number of abandoned coal mines has gradually increased, and the mine water has polluted and damaged the surrounding water system, thus affecting the production and life of local residents. For example, there are 298 coal mines distributed in the Jinci Spring area, Shanxi Province, China. The amount of the mine water discharge in this area can reach 24.68 million m^3 each year, which seriously affects the health of residents [6]. After the

Hongshan and Zhaili coal mines were abandoned, the groundwater in goaves could not be drained, causing a rise in the water table. The accumulated water in the goaves then polluted the karst water in this region [7]. Around the famous Niangziguan Spring area, groundwater in abandoned coal mines increased the concentration of sulfate ions and increased water hardness [8]. The Yudong River in Kaili City, Guizhou Province, was seriously polluted by acid mine drainage from abandoned mines [9]. In central Montana, the Madison aquifer feeds two very large natural springs at either end of the Great Falls-Lewistown Coal Field, named Giant Spring and Big Spring, and it has been documented that the abandoned coal mine has caused localized contamination in the Madison aquifer from AMD water [10].

In order to protect the karst water from pollution, different options have been adopted to eliminate pollution sources and pathways. The karst springs within the influence range of abandoned coal mines have been scientifically investigated to understand the flow characteristics of spring water and to delimit the protection area. Kakaroglu proposed the establishment of a karst water environment protection zone through scientific planning, investigation, and analysis [11]. Hao et al. divided the Niangziguan Spring into 3 areas with 11 intersections and discharge areas as first-grade protection zones, the supply basin as a second-grade protection zone, and the dry area with a less supply as a third-grade protection zone [12]. Giudici established a flow model in a karst aquifer, and Javier Valdes-Abellan established a karst aquifer model (KAGIS model) based on GIS to simulate the movement and influence of pollution [13,14]. Jiang et al. established an environment impact model of water in goaves, taking the Jinci Spring as an example, and proved that the water near the coal mine was easily affected by the water from goaves [15].

The pollution source for a polluted water area should be cut off first, and then all kinds of scientific methods can be used to purify the pollution. At present, mine wastewater treatments mainly comprise chemical, physical, and biological approaches. The most common method in China is the use of neutralization technology with limestone, fly ash, and red mud as materials. In addition, there are microbial, electrochemical, membrane separation, chemical precipitation, and artificial wetland technologies [16–20].

In order to stop coal mine water from recharging karst water, it is necessary to set a protective coal pillar with a certain thickness [21]. The mechanism of pollution should be analyzed and studied through geological investigation. In order to reduce the discharge of the polluted water to complete source control, the pathway between the karst and goaf water should be blocked. Some methods, such as pathway blocking, vertical curtain grouting, and goaf filling, can be carried out in regional treatments. Source control combined with grouting is another recent mode of treatment [22].

A monitoring network of groundwater quality and pollution has been established to evaluate the dynamic changes in water quality and quantity in order to provide references for protecting karst water. Researchers have put forward many recommendations and measures, including water resource management, reasonable water resource planning, optimal water resource allocation, groundwater control, pollution source control, and dynamic groundwater monitoring [23].

The geological conditions and groundwater runoff mode in the karst areas of Southwest China are special, so it is of great importance to protect karst spring water through study. Peng et al. stated that it is necessary to take an underground basin as a unit instead of a karst basin as a unit in order to investigate the characteristics of karst aquifers [24]. Various methods need to be comprehensively adopted in karst areas, such as hydrogeological surveys, geophysical explorations, hydrogeological drillings, tracer tests, cave detection, and dynamic monitoring. Geophysical explorations are always used to detect complex karst caves, and common techniques for this detection include the electromagnetic, electrical sounding, and multi-electrode resistivity methods. Hydrogeological drilling is used to understand lithology, geological structure, and groundwater resources. A tracer test can trace and determine the source of pollutants and flow rate in these systems before estimating the recovery time. The cave detection method can be adopted to investigate the features

of caves, to analyze the relationship between cave shape and geological structure, and to finally learn the direction of groundwater flow and the connection between an underground pathway and karst water [25]. Dynamic monitoring can be used to analyze the hydraulic connection between boreholes through the accurate, real-time monitoring of water levels in mined-out areas. Ultimately, different methods should be selected by considering geological and natural conditions.

The study area is located in Qingganglin Village, about 2.5 km southwest of Dafengdong Town, Kaili City, Guizhou Province. There are more than 100 abandoned coal mines in Kaili City, Guizhou Province, and acid mine drainage has seriously polluted Yudong River [9]. The Longdong Spring, which is an important source of drinking water in the village, was polluted after heavy rainfall on 27 June 2017. After that, pollution and recovery phenomena appeared several times. The Longdong Spring had become a "red spring" in the rainy season, which has seriously affected normal production and life.

In order to understand why Longdong Spring was polluted, investigations have been carried out since July 2017 with hydrogeological surveys, geophysical surveys, and borehole drilling to characterize the lithologies, water levels, and water quality of the karst aquifers. The authors of this study investigated the vertical and horizontal distributions of water abundance to identify the main source of pollution. Following the hydrogeological survey, the authors of this work analyzed pollution sources and pathways; then, they formulated recommendations for pollution control. The main goal of this research was to investigate the reasons for spring pollution in a karst area. As the pollution of the Longdong Spring is typical and representative in Guizhou Province, this investigation can provide reference for the study of spring pollution in karst areas.

2. Materials and Methods

The authors of this investigation focused on the source and the pathway of pollution based on the characteristics of the study area. First, a preliminary investigation of the study area was carried out based on data collection and analysis. Second, special methods, such as hydrogeological surveys, geophysical surveys, drilling, cave detection, and tracer tests, were used to explore the aforementioned pollution sources and pathway.

2.1. Study Area

The study area is dominated by a karst landform, with high terrain in the northeast, low terrain in the southwest and a slope of 5–60°. The highest elevation is +973 m, and the lowest elevation is +807 m. The terrain is steep due to the uplift of the Yunnan-Kweichow Plateau and river cutting. The vegetation in the area includes evergreen broad-leaved forests, coniferous forests, shrubs and grass, with a vegetation coverage rate of 53.28%. This area belongs to the subtropical humid climate zone with an annual average temperature of 13.6–16.2 °C July is the hottest period with an average temperature of 23.2–25.8 °C. (http://www.kaili.gov.cn, assessed on 24 August 2021) January is the coldest month with an average temperature of 2.6–5.2 °C. There are four distinct seasons, mild climate, abundant rainfall, no severe cold in winter, no severe heat in summer, and a long frost-free period—thus showing obvious monsoon climate characteristics. The average annual rainfall is 1240.1 mm, which is suitable for the development of agriculture, forestry and animal husbandry. The surface rivers are well developed and abundant in the study area. The major surface creeks include Dafengdong gully, Xiaohe River, and Gebaochong gully. The Longdong Spring is the main supply source of the Xiaohe River, which originates in the southeast of the mining area and flows into the Baishui River. Figure 1 shows the location of the Longdong Spring. It is in a terrace slope, higher in the northwest and southeast with the highest point in the northwest of +1137 m asl. The southwest, middle and northeast areas are relatively low, with the highest altitude of +1100 m and the lowest altitude +855 m.
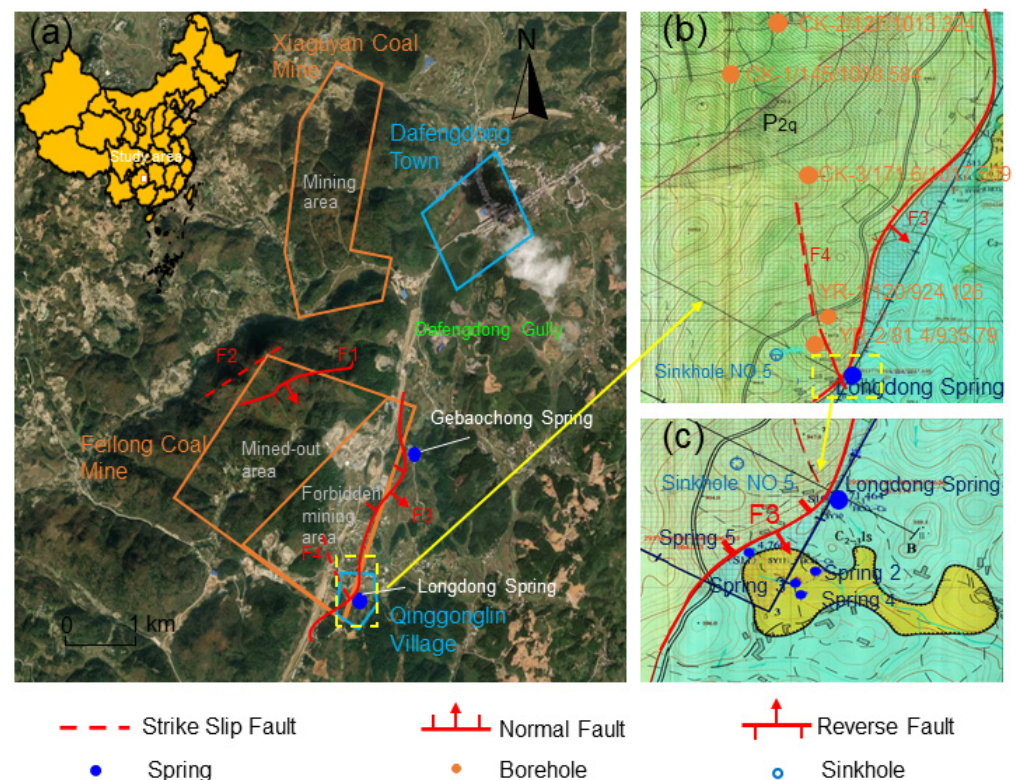
Figure 1. Location of the study area: (**a**) distribution of the main relevant areas; (**b**) location of the main boreholes; (**c**) Longdong Spring and surrounding springs.

The strata sequences in the study area include the lower Permian Liangshan Formation, the middle Qixia Formation, the Maokou Formation and the Quaternary.

The Quaternary (Q) consists of clay, sand and gravel with an average thickness of 14.22 m and a poor hydraulic conductivity. The Permian Middle Maokou Formation (P_{2m}) has a thickness ranging from 20.8 to 91 m and an average of 52.6 m. It is composed of gray and white, thick, layered massive cryptocrystalline limestone that is filled with a few flint nodules. Dissolved pores, caves, and fissures have developed and are partially filled with calcite. According to borehole drillings, three layers of karst caves have developed. Two layers of karst caves are in the middle part, with a height of less than 1 m, and they are filled with fine sand. Another karst cave layer has developed at the bottom with a height of 1.2 m, and it is filled with clay mud. The Permian Qixia Formation (P_{2q}) has a thickness ranging from 44.8 to 72.5 m and the average thickness is 56.65 m. It is composed of dark gray, gray black medium-thick limestone, containing clayey, organic matter and flint nodules, with clayey bands in some parts. A small amount of brown calcareous shale is distributed in the lower part. In this formation, dissolved pores and fissures only developed at the bottom, most of them are closed and filled with calcites, and oily matter is partially distributed. The Lower Permian Liangshan Formation (P_{1l}) consists of clayey limestone, gray clayey shale, coal seams and white bauxite shale. Though our borehole drilling did not completely expose the entire formation, the drilling thickness in this formation was found to reach 16.60 m. The thickness of the coal seam was found to vary from 0.6 to 3.3 m. The CK-1 (Figure 2) and CK-2 boreholes exposed goaves with cutting heights of 1.7 and 2.2 m, respectively.

The study area is geologically located in the east-middle part of the Guiding North-South structural transformation zone in the southern Qiannan platform of the Yangtze quasi platform. It forms a groove-shaped fold with a wide anticline and a tight syncline. The Dafengdong syncline is located in the northwest side of the study area, strikes N19°E, and extends about 22 km. The occurrence of the north west limb is 118°∠29° while the south east limb is 290°∠10°. There are four faults in this area. F1 is located in the northwest

of the Feilong coal mine. It is a normal fault with an extension of 2.9 km in the mine, dipping to 105° with a dip angle of 77°. F2, developed in the northwest of the mining area, is a strike slip fault with a dip direction of 275°, a dip angle of 82°, and an extension of about 700 m. F3 passes through the Qingganglin Village, Dafengdong Town in the southeast of Feilong Coal Mine, extending 4.4 km. It is a reverse fault with a dip angle of 70°. F4 is located in the north of Qingganglin Village, strikes NNW-SSE, and has an extension of 670 m with unknown occurrence.

System	Formation	Thickness (m)	Depth (m)	Column	Lithology
Q		5.4	5.4		**Sand, gravel, sediment**
P₂	P₂m	52.4	57.8		**Limestone** Gray-white thick layered massive cryptocrystalline limestone is filled with a few flint nodules. Dissolved pores, caves, and fissures develop and are partially filled with calcite. Two karst caves in the middle part are filled with fine sand with a drilling depth of 33.5 m and 40.7 m, respectively. At the drilling depth of 56.6 m, there is another karst cave with a height of 1.2 m.
	P₂q	72.5	130.3		**Limestone** Dark gray, gray-black medium-thick limestone contains argillaceous, organic matter and flint nodules. Dissolved pores and fissures only develop at the bottom, but most of them are closed, filled with calcite, and oily minerals can be seen. **Water-conducting fractured zone** is at the depth of about 123 m with a height of 10 times goaf height
P₁	P₁l	11.9	142.2		Argillaceous limestone, gray argillaceous shale are concentrated in this formation. **The depth of the goaf:** 142.2-142.9 m
		1.7	143.9	goaf	
		1.1	145.0		

Figure 2. Stratigraphic column in borehole CK-1.

Hydrogeological features of the study area were investigated in this study. The principal karst forms mainly include stone teeth, karst trenches (troughs), and karst caves. The hollows are distributed in a beaded shape in the watershed area. The bottoms are covered with clay and often embedded with sinkholes and funnels (Figure 3a). It is a recharge zone for underground karst pathway.

Figure 3. Investigation methods: (**a**) karst core sample from borehole YR-1; (**b**) water quality detection; (**c**) pollution in the Longdong Spring; (**d**) diving exploration in Sinkhole No.5.

2.2. Hydrogeological Survey

Geological and geomorphic features, surface water types, vegetation coverage, site types, and human activity were observed in the study area. The hydrogeological conditions in the study area were analyzed based on previous hydrogeological information, and a further survey was carried out in this study [26].

In order to investigate the reason for the pollution of the Longdong Spring, this survey started in July 2017 to further study the underground karst water in the research area. Nine hydrological boreholes (seven for groundwater level observation in the goaves and two for karst groundwater level observation), with a total of drilling length of 937 m, were created. In addition, we conducted 4 tracer tests, 2 cave detections, a special hydrogeological survey in a 3.84 km^2 area, and 18 engineering measurement points, as well as corresponding water quality monitoring, geological cataloging, and well logging.

2.3. Hydrological and Geophysical Exploration

The transient electromagnetic method combined with the direct current electric method was used to detect water-rich areas, the distribution of the coal mine goaf, and polluted pathways. A V8 multi-function electrical instrument produced by Canada Phoenix Company and the Large Fixed Loop Source Transient Electromagnetic Method were used in this exploration.

2.4. Hydrogeological Borehole Drilling

Drilling provided the basis to characterize the distribution of aquifers or aquifuges, as well as the recharge and discharge and migration of groundwater in the study area through the characterization of geological structures, strata consequences, aquifer characteristics, and coal seam roof and floor thicknesses. A total of nine boreholes were drilled, with a total area of 1037.4 m. Among them, seven boreholes were for goaf groundwater surveys, and two were for karst groundwater surveys. A water level monitoring system with five

sub-stations was established. In each borehole, geological logging and a downhole TV were used to obtain the strata data. Figure 4a, b shows the water-conducting fracture development in borehole CK-1 in the depths from 123.6 to 124.2 m and from 139.1 to 139.7 m, respectively.
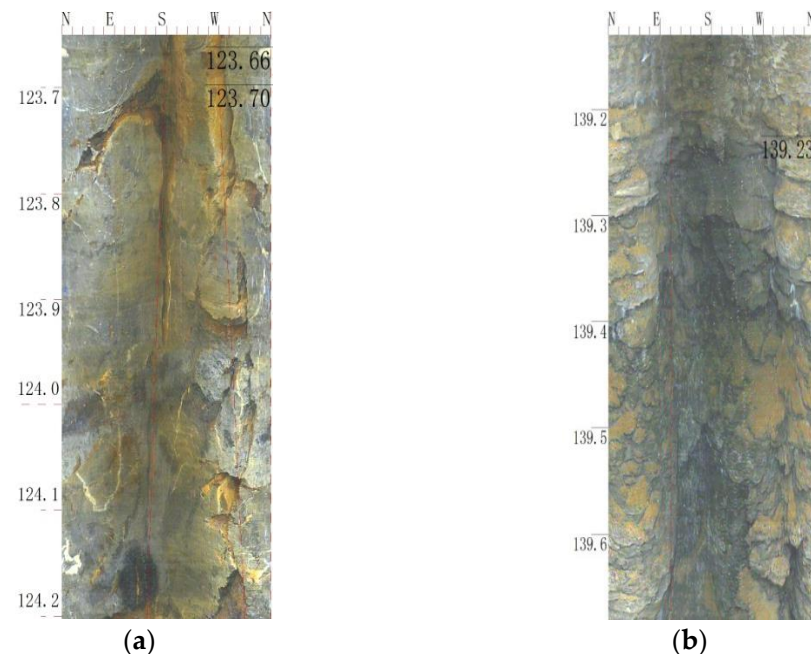

(a)   (b)

Figure 4. Water-conducting fractured zone detected in borehole CK-1: (**a**) at depth 123.6 to 124.2 m; (**b**) at depth 139.1 to 139.7 m.

2.5. Tracer Test

A tracer test was used to investigate the hydraulic connection among sinkholes, boreholes, goaves, and the Longdong Spring.

When the flow in the sinkhole and the Longdong Spring was stable and the water was clear, the test could start. NaCl and fluorescein ($C_{20}H_{12}O_5$) were selected as tracers. Then, 50 kg of salt, 2 kg of fluorescein, several sampling bottles, several labels, 4 portable pH/TDS/EC detection instruments, 4 BEHRINGER 7500 photometers, 200 pieces of 7500 chloride quantitative reagents, a stopwatch, and a flowmeter were prepared. Next, 50 kg of dissolved edible salt and 2 kg of fluorescein were placed at the launch point within 10 min. The flow rate was tested in the launch point of sinkhole.

The observation started at the same time at each observation point. Before the tracer was placed, the portable pH/TDS/EC detector was inserted into the water to record the initial data. The original water sample was collected and the chloride concentration in the original sample was detected by a BEHRINGER 7500 photometer. After the tracer was placed, the electrical conductivity (EC) in the water was monitored in real time. The water samples were collected and the chloride concentration in the water samples was detected by a BEHRINGER 7500 photometer with a sampling interval of 20 min. The observation interval decreased to 10 min when the water color changed. The interval returned to 20 min when the water started to be clear again and the EC and chloride concentration continued decreasing. The observation stopped when the water became clear again and the EC and chloride concentration declined to the initial values and stabilize for 3 h. Flow rate was recorded again at the end of the test. Springs 2, 3, and 4 were auxiliary observation points. If no tracer was observed or the spring cut off during testing, the observation could be extended. A total of 4 tracer tests were performed. The tracer-released points were Sinkhole No.5 and boreholes CK-1, CK-2, and YR-2. The observation lasted for 50 days.

2.6. Cave Detection

Cave detection in the mouth of the Longdong Spring showed that water flows out from the Longdong Spring mouth all year round. The opening is narrow but has a large flow rate. The water level in the cave is high and the space inside is unknown. At the same time, it has been speculated that there are many large reservoirs in the cave. Therefore, the diving and boat methods were used to detect the direction of water flow and karst cave development to track the pollution source and pathway (Figure 3c).

Cave detection for Sinkhole No.5 was divided into two parts. First, we tracked the direction of underground river flow to detect whether it eventually flows into the Longdong Spring. If it was found to eventually merge into the Longdong Spring, it would be necessary to clarify the merge position. If it was not found to merge into the Longdong Spring, it would be necessary to determine the direction of the underground river and the development of the karst cave, as well as to analyze the discharge location. Second, we traced karst development and the recharge source of the underground river (Figure 3d).

The detection of two caves near the main shaft of the Feilong coal mine showed that water at the entrance of cave is shallow. There is no water at the exit, and the space in the cave is open. Downstream detection was used to track the flow direction and determine the position of the cut-off. Based on this, whether the cave is connected to the Feilong coal mine and whether it supplies the Feilong coal mine goaves were determined.

2.7. Groundwater and Rainfall Monitoring

Automatic groundwater level monitoring equipment was installed in 5 boreholes: CK-1, CK-2, CK-3, YR-1, and YR-2. Boreholes CK-1 and CK-2 were in the goaf in the middle of the mine, CK-3 was in the mine sumps in the southeast of the mine, and YR-1 and YR-2 were in the footwall of the F3 fault in northwest of the Longdong Spring. The monitoring data could be transmitted to the internet in real time. The monitoring frequency was 4–5 times per hour or adjusted according to needs. Real-time monitoring and comparative analysis could indicate the hydraulic connection among boreholes and goaves.

Water quality monitoring was carried out a total of 326 times from May 2018 to March 2019, including 297 instances of the on-site monitoring of polluted water in the Longdong Spring, 8 instances for sinkholes, 5 instances for boreholes, and 12 instances for caves. The type of pollution in the Longdong Spring was clarified by the monitoring.

The rainfall monitoring was carried out with a rainfall gauge from May 2018 to investigate the relationship between Longdong Spring water pollution and precipitation. Rain was monitored for a total of 51 times in this work. The beginning and ending times and rainfall were recorded. The relationship between the flow rate and pollution of the Longdong Spring was analyzed to investigate the pollution source.

3. Results

3.1. Hydrogeology

The underground karsts in the study area were found to be dominated by sinkholes, karst caves, and karst pipelines. They are multi-layered and have different scales. Their extension direction was found to be controlled by rock strata and structural fractures. They are the main pathways for recharge and runoff of groundwater. At the bottom of the Maokou Formation (P_{2m}), we found a karst cave larger than 1 m. The bottom of the karst cave was filled with mud, and the main karst pathways in the study area were distributed in the Maokou Formation (P_{2m}). The dissolution rate of the Qixia Formation (P_{2q}) was found to be much smaller than that of the Maokou Formation (P_{2m}) because of widely distributed clayey material in the Qixia Formation (P_{2q}). In addition, dissolved pores and fissures were mainly developed at the bottom and filled with calcite, resulting in a relatively poor water abundance compared to the Maokou Formation (P_{2m}). The karst water level in the main aquifer was found to be located 40 m below the top interface of the Qixia Formation, with an elevation ranging from +867.69 to +935.40 m. The groundwater

flows from the northwest to southeast before finally discharging into the karst springs in the southeast.

The investigation results also revealed the recharge, flow-off, and drainage conditions of the aquifers. Atmospheric precipitation recharged karst groundwater. The study area can be divided into two hydrogeological units, the north one and south one, with the ridge in the west of Bailachong Village as the watershed. After precipitation in the north unit, the groundwater flows out from the gully in the Feilong main shaft and drains from the Yunxi cave to Dafengdong town. We found underground rivers and surface water in the Yunxi cave. The elevation of the entrance port in the main and auxiliary shafts of the Feilong coal mine is about +930 m. After the surface water is collected into the Feilong coal mine gully, it flows to Dafengdong Town through the cave. The south unit is the southeastern part of the mining area, with an elevation of +860–880 m. As the main collection and runoff zone of groundwater, the Longdong and other springs are exposed in this unit.

3.2. Pollution and Monitoring

Qingganglin Village is located about 2.5 km southwest of Dafengdong Town in Kaili City. There are four springs and three sinkholes in the gully area of the village. The Longdong Spring (Spring 1) is at +863.25 m asl, with a flow rate of 200–1200 m^3/h in the wet season and 90–400 m^3/h in the dry season. It is a perennial spring with an oval mouth and a trend of N50°E. This spring is the main source of water for production and life in the village, serving more than 2000 people in the village and downstream. Springs 2, 3, and 4 are seasonal springs with a flow rate of generally less than 50 m^3/h; they are even dry during the dry season.

Pollution in the Longdong Spring first occurred three days after a heavy rainfall on 27 June 2017, and the water quality suddenly deteriorated on 30 June 2017. The water was turbid and contained a large amount of red suspended solids. Red sediment could be found where the water flows (Figure 3c). There had never been any pollution before. The spring became clear again on 14 July 2017 (Figure 5a). Until November 2017, the Longdong Spring was polluted and recovered several times. However, no relevant data could be gathered due to the short period of pollution. There was no pollution in the Longdong Spring from December 2017 to April 2018. On 22 April 2018, the Longdong Spring was polluted again, and it lasted until 24 April. Pollution continued from May 2018 to the end of August 2018. After August 2018, pollution and recovery phenomena occurred again. Figure 5b shows the changes of the concentration of Fe and Mn ions. pH was found to be less than 7, and the concentration of Fe and Mn ions in the spring water were found to exceed the Standards for Drinking Water Quality (China), which states that the concentrations of Fe and Mn cannot exceed 0.3 and 0.1 mg/L, respectively.
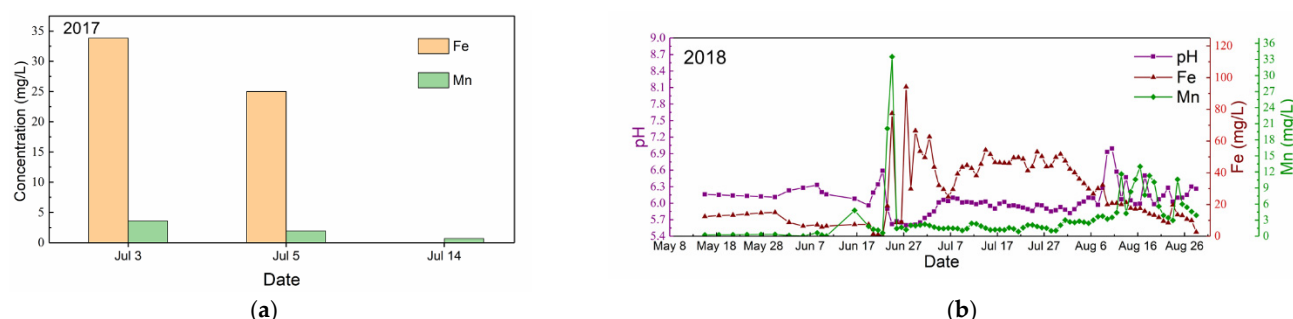

(a)　　　　　　　　　　　　　　　　　　　　　　　　　　(b)

Figure 5. Pollution condition in the Longdong Spring: (**a**) in 2017 and (**b**) in 2018.

3.2.1. Relationship between Flow Rate and Rainfall

Figure 6 shows the relationship between spring flow rate and rainfall based on monitoring data. Rainfall was found to be concentrated in the middle of June, followed by August and September. There were three rainstorms and several light and moderate rainfalls during this period. The first period when the flow rate changed obviously was from

20 June to 30 June. The quantity of rainfall was 86.26 mm on 20 June and 138.15 mm on 21 June, and the accumulated rainfall even reached 218.41 mm on 22 June. Consequently, a maximum flow rate of 5901.65 m^3/h of the Longdong Spring was observed on 23 June. The rainfall from 23 August to 24 August was 43.93 mm, and the flow rate of the Longdong Spring increased from 118.24 m^3/h on 22 August to 724.54 m^3/h on 24 August. This showed that the duration of monitoring was a rainy period, with the largest rainfall from June to July, followed by August and September. The increase in the flow rate of the Longdong Spring lagged about 24 h behind the rainfall. The flow rate of the Longdong Spring was found to be greatly affected by short-distance recharge.
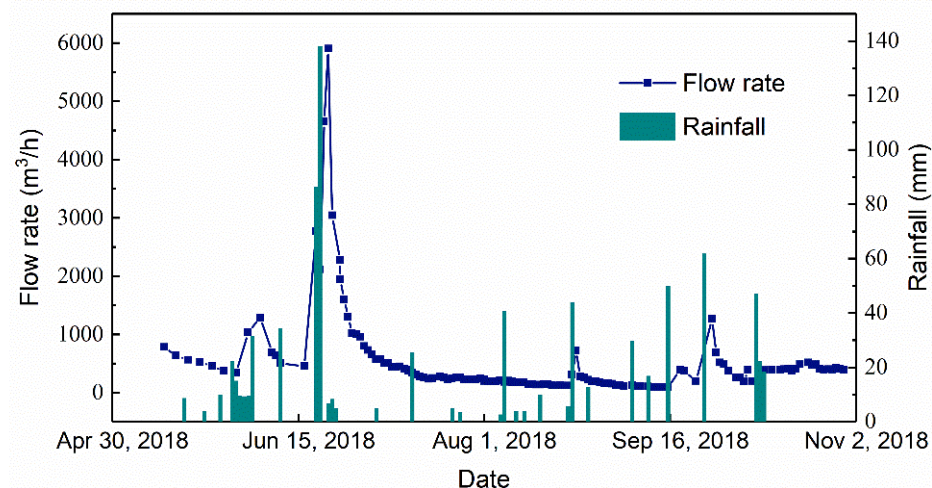

Figure 6. Relationship between spring flow rate and rainfall.

3.2.2. Relationship between the Concentration of Fe and Flow Rate

Figure 7 shows that the concentration of Fe ions decreased with increasing flow rate due to rainfall at the very beginning. On 6 June, the concentration of Fe was 6.4 mg/L, which corresponded to a flow rate of 1289.15 m^3/h. The concentration of Fe ions was 1.37 mg/L, with a corresponding flow rate of 2456.53 m^3/h on 21 June. On 23 June, the concentration of Fe was 0.3 mg/L and the flow rate was 5901.65 m^3/h. The maximum concentration of Fe lagged about 48 h behind the maximum flow rate. The concentration of Fe fluctuated in the early stage from 23 June to 8 July, with a maximum value of 97.8 mg/L and a minimum value of 0.3 mg/L. It can be speculated there is not only acid mine water with iron, manganese, and sulfate in the goaves of the Feilong coal mine but also mine water with a low pollution concentration. This also implies that when the amount of rainfall is small, there is poor hydraulic connectivity and static or very slow water flow inside the goaves. The concentration of Fe was found to be relatively small when the flow rate was less than 200 m^3/h. From 9 July to 3 August, the concentration of Fe was basically stable at 35–55mg/L due to the decline of flow rate. It is speculated that the water in the goaf is in a confined state, so the water level drops slowly. The acid mine water in the goaves drained out, mixed with the clean water in the pathway, and finally discharged into the Longdong Spring. This resulted in a stable concentration of Fe in the spring water. From 3 August to 22 August, the concentration of Fe rapidly dropped from 38.8 mg/L on 3 August to 8.6 mg/L on 22 August, with a slow drop of flow rate. It can be inferred that the mine water was in an unconfined state in the goaves, which resulted a rapid decrease in the outflow of mine water and a rapid decrease in the concentration of Fe. After 28 August, the concentration of Fe did not exceed 10 mg/L, which showed that the mine water in the goaves was diluted and the concentration of Fe was reduced due to the recharge of groundwater in the rainy season. In addition, the recharge rate was greater than the production rate of acidic water, resulting in a downward trend in the concentration of Fe in the spring water.
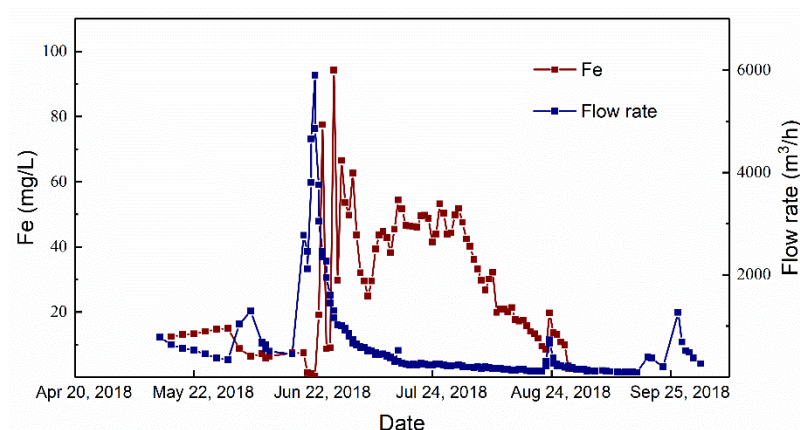
Figure 7. Changes of flow rate and concentration of Fe.

The pollution was found to be serious in the rainy season and light in the dry season. In the early stage of pollution, the concentration of Fe fluctuated; in the middle stage, the concentration stayed stable for a long time, with a rapid decrease in spring flow rate; after that, the concentration of Fe rapidly decreased, with a slow decrease in flow rate. There were several occurrences of rapid pollution and recovery in the rainy season.

3.2.3. Relationship among Fe/Mn/SO_4^{2-}

Figure 8a shows that the concentration of SO_4^{2-} had a positive correlation with that of Fe. For example, the concentration of Fe was 15 mg/L and the concentration of SO_4^{2-} was 350 mg/L on 30 May. The concentration of Fe was 6.4 mg/L when the concentration of SO_4^{2-} decreased to 190 mg/L on 6 June.
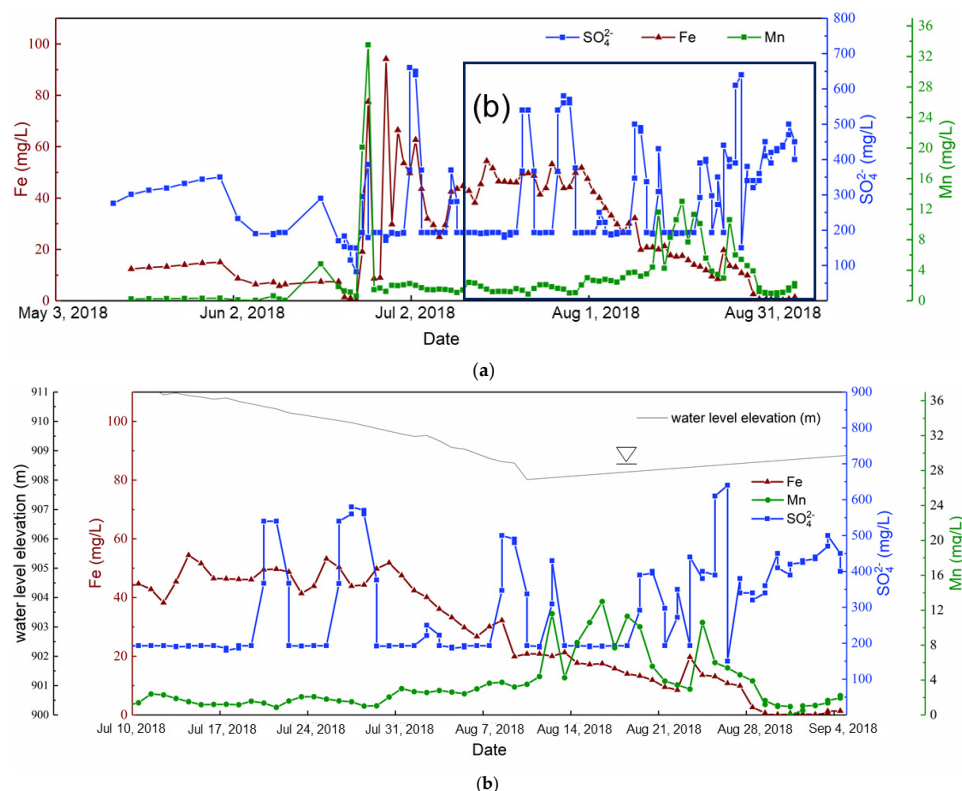

(**a**)

(**b**)

Figure 8. (**a**) Concentration of Fe/Mn/SO_4^{2-}. (**b**) is the part enlarged in (**a**).

3.3. Pollution Source Tracking

The study area houses the Feilong and Xiaguyan coal mines (Figure 1a).

The Feilong coal mine has an area of 3.16 km², with a production capacity of 90,000 t/a. An inclined shaft has developed and a room and pillar method has been used in the coal mine. The mining coal seam is seam M1 in the Permian Liangshan Formation with a thickness of 0.8 to 1.3 m. The minimum mining elevation was found to be +880 m asl, and mining has been conducted in the west and north areas. The mine head of the Feilong coal mine is +934.6 m asl; this mine was closed in March 2017 after more than 10 years of mining. The goaves were found to be mainly distributed in the north and west of the mine, with an area of 0.3 km² according to the survey statistics. The height of the water-conducting fractured zone was detected by borehole TV to be generally 6.57–10.91 times the cutting height and to reach the karst area at the bottom of the Qixia Formation. Before the Feilong coal mine was abandoned, there was little water in the roadways during operation because a drainage of 10–40 m³/h was discharged to the ground ditches in the mine. The drainage water was red, and the ditches turned yellow, which was similar to the pollution phenomenon in the Longdong Spring. There was only a small amount of accumulated water in the mine due to continuous drainage, which stopped after the mine was abandoned. The karst water in the roof of the coal seam has been continuously supplied through the water-conducting fracture zone; the mine water was found to be rapidly recharged by karst water after heavy rainfall, which caused a rise in the water level in the goaf, and then the mine water could connect the Longdong Spring along pathways, resulting in spring water pollution. In the dry season, the water level in the goaf is dropped, and the groundwater in the goaf cannot enter the karst fissures or pathways. Therefore, the spring water is not polluted in the dry season (Figure 9). The chemical analysis results of the accumulated water in the goaf of borehole CK-1 indicated that the pollution of the Longdong Spring is consistent with the pollution characteristics of the coal mine wastewater, which also indicated that the pollution source is the water from the coal mine.
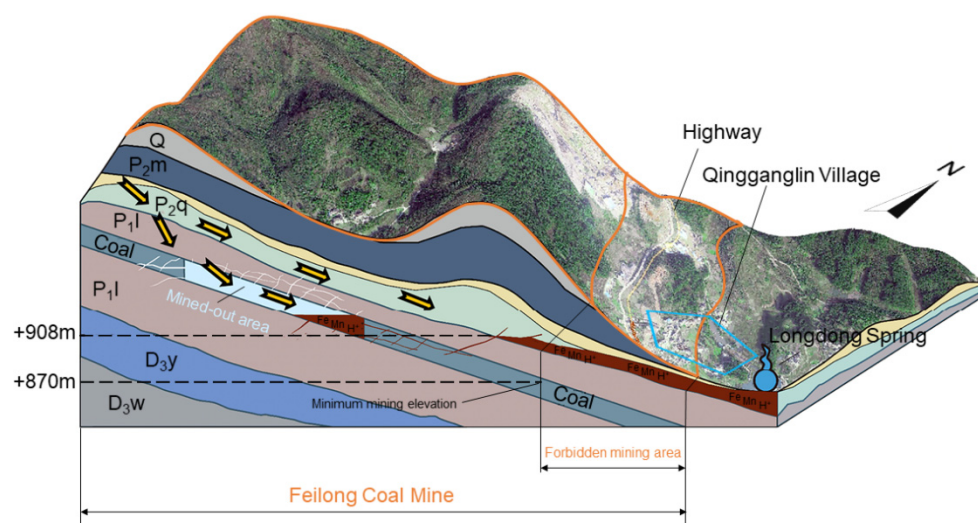

Figure 9. Mine water flows from the coal mine into the Longdong Spring.

The Xiaguyan coal mine is located in the northwest of Qingganglin Village, with an area of 1.40 km² and a production capacity of 90,000 t/a. The coal mine has developed an inclined shaft and room-pillar has been mined. The mining area is in the south of the mine. The coal seam has a thickness ranging from 0.6 to 1.2 m in the Permian Liangshan Formation. The entrance of the mine is at an elevation is +922.4 m asl, and the mining was carried out from +900 to +850 m. The mine was closed in April 2017, and it was permanently abandoned on 23 August 2017 after 10 years of operation. The mine water was pumped to the surface before abandonment. In the east of Feilong coal mine and the southeast of Xiaguyan coal mine, three springs in the Gebaochong Spring group were exposed (Figure 1a). Turbidity had previously occurred in the three springs due to the sand and mud carried by surface water after precipitation. This phenomenon is not similar to the

pollution in the Longdong Spring. Since the Gebaochong Spring group is located between the Xiaguyan coal mine and the Longdong Spring, if the Longdong Spring was polluted by the mine water from the Xiaguyan coal mine, the Gebaochong Spring group would be polluted first. However, the Gebaochong Spring Group has never been polluted in recent years. Even after the Longdong Spring was polluted, the Gebaochong Spring group remained clear. In addition, the Dafengdong Karst Gully located between the Feilong and Xiaguyan coal mines is the erosion base level in the region (Figure 1a). Groundwater in both the northern part of the Feilong coal mine and the southern part of the Xiaguyan coal mine was found to be discharged into the Dafengdong Karst Gully. Then, the water merges into the Dafengdong Karst Gully and runs off from the southwest to the northeast towards Dafengdong Town, which indicates that the Longdong Spring is less likely to be polluted by drainage from the Xiaguyan coal mine.

3.4. Groundwater Accumulation in Abandoned Mine Goaves

Figure 10 shows three-dimensional result according to transient electromagnetic survey, where blue and red represent relatively low and high resistance areas, respectively. The suspected goaves are distributed in the west and northwest of the study area. The goaves of the Feilong coal mine are in the west of this area (with a relatively higher elevation), which are also characterized by borehole drilling and investigation. Meanwhile, the northwest area houses the goaves of the Xiaguyan coal mine. The suspected groundwater accumulation zones in the goaves are in the north and center of the study area with a relatively low terrain, which made it even more susceptible to karst water recharge and groundwater accumulation after the coal seam was mined out. The CK-1 borehole revealed the existence of a goaf that is filled with groundwater, so the geophysical survey results were verified (Figure 10).
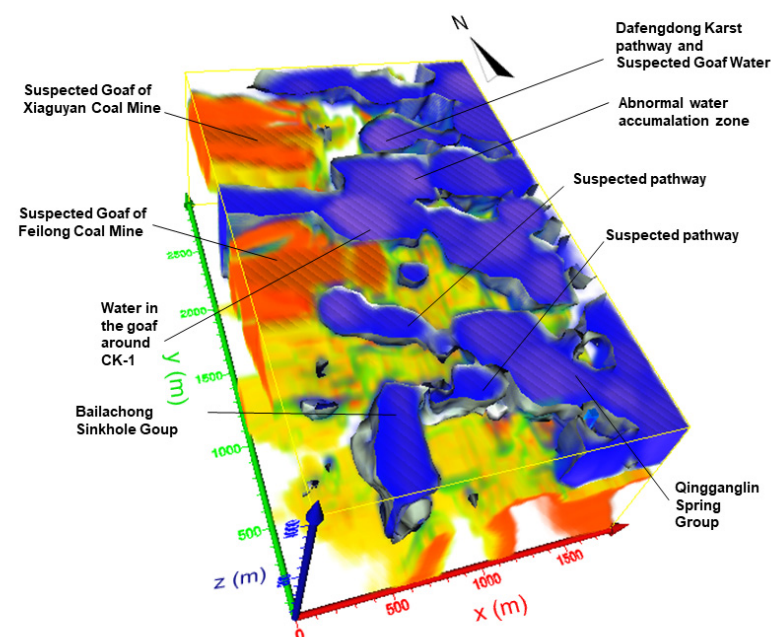

Figure 10. Results of transient electromagnetic survey.

3.5. Polluted Pathways

3.5.1. Fractured Pathway

The tracer test and chemical indices in fractured pathway led to a clear conclusion that there was a poor connectivity between groundwater in the goaves near boreholes CK-1 and CK-2. Pollution was found to be concentrated in the area near borehole CK-1, while pollution was found to be light in the area near borehole CK-2. The tracer needed to travel for a long time due to a long distance between the launching point and the Longdong

Spring. We could not determine whether there was a connection between the CK-1 and the Longdong Spring due to limited time and testing abilities.

3.5.2. Sinkhole

The tracer test was used to investigate the hydraulic connections between Sinkhole No.5 and the Longdong Spring—especially Springs 2, 3, and 4—to determine the pathway of pollution. The observation points are shown in Figure 1c. Sinkhole No.5 was found to have an almost elliptical opening, with a major axis of 25 m, a minor axis of 15 m, and a major axis direction of N35°E. It is located at an elevation of +897.64 m, with a depth of about 15 m. There is a perennial underground river at the bottom of the sinkhole. The water quality of the underground river and Springs 2, 3, and 4 did not obviously change when the Longdong Spring was polluted. After the tracer was put into Sinkhole No.5 at 3:50 pm on May 18, the chloride concentration started to change, and the EC began to increase at minute 252 (Figure 11) in the Longdong Spring observation point. The chloride concentration and EC reached their maxima at 580 min and then slowly decreased until returning to normal values. The color of the water sample in the Longdong Spring obviously changed at 22:27 on May 18. At the same time, the chloride concentration and water color in Springs 2, 3, and 4 did not show obvious changes. It could be inferred that the underground river of Sinkhole No.5 has a hydraulic connection with the Longdong Spring. Sinkhole No.5 supplies the Longdong Spring through an underground river, but it has poor hydraulic connections with Springs 2, 3, and 4. Figure 11 shows two peaks and a long-lasting decline. It can be inferred that there are at least three large ponds in the underground pathway between Sinkhole No.5 and the Longdong Spring. The pathway between Sinkhole No.5 and Longdong Spring is not flat because the concentration of chloride and EC was found to fluctuate in a small range. The tracer test results showed that that the regional reverse F3 fault is not a complete water barrier. Groundwater could connect the ground surface through fissures in the fractured zone and form the Longdong Spring. The underground river of Sinkhole No.5 was still clear after precipitation, while the Longdong Spring was polluted by overflow from the goaves. This shows that there is a pathway between Sinkhole No.5 and the Longdong Spring that conducts coal mine water into the Longdong Spring and causes pollution. Some of the water in the underground river of Sinkhole No.5 is mainly pumped and used by people upstream, and the rest is supplied to the Longdong Spring, which was found to account for 70–85% of the discharge of the Longdong Spring.
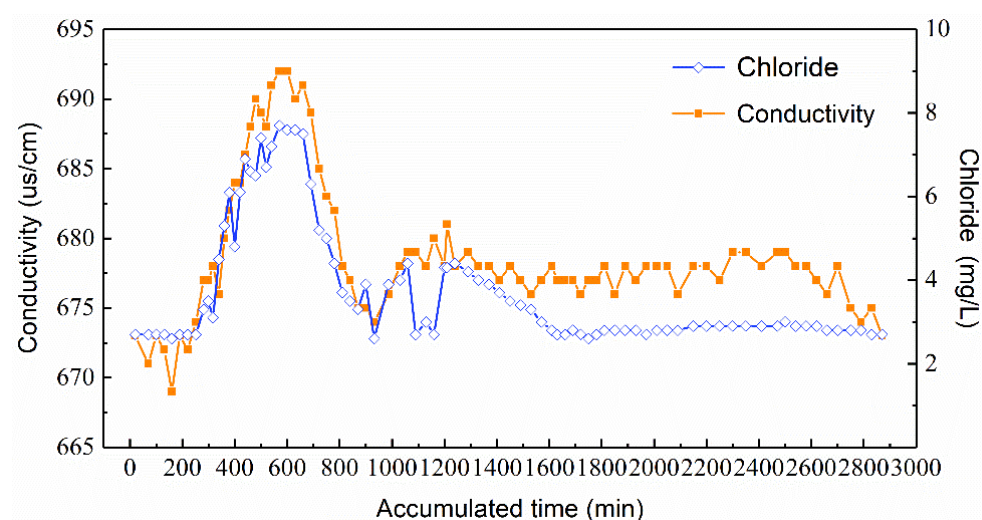

Figure 11. Changes in the conductivity and concentration of chloride.

3.5.3. Cave Detections

Sinkhole No.5 is beside provincial Highway 308 at the entrance of Qingganglin Village (Figure 1c). The tracer test proved that Sinkhole No.5 is connected to and might provide a pollution source pathway to the Longdong Spring. The downstream traceability and an upstream exploration were carried out to investigate the locations of contaminated pathways.

The exploration showed that Sinkhole No.5 is a collapsed shaft with a cone shape below and a depth of 15 m. The collapsed, accumulated rock mass extends to the underground river. It could be judged from the location of mud attachment at the steep slope that the highest water level could reach 4 m above the riverbed. The underground river flows from the west to the east, with a width of 1 m and a height of 3 m. The riverbed is relatively shallow, with distributed gravel, and the current is turbulent at the entrance. The river gradually becomes deeper towards the east, the water surface is smooth, and the flow speed is small. The riverbed is deposited with fine sand and a small amount of gravel. The water channel becomes narrow after extending 25 m to the east, with a height of 50 cm from the water surface to the roof. At point A (Figure 12), clay attaches to the left wall near the water surface and the water depth is 0.5 m. There is also a small meandering channel on the wall 20 m behind point A, which finally merges with the underground river at point B. Red clay is attached to the entire wall in this section, and the water depth is 1 m. After point B, swimming is necessary for exploration because the underground river becomes deeper and deeper. Shallows were found to be irregularly distributed, and the depth of the river is 1 or 2 m, with a minimum height from the water surface to the cave roof of 2 m. We found a leakage area on the wall of the cave, though without fractures. Point C is 3 m away from the position of the leakage where the depth of the river increases sharply. After advancing 10 m, the tunnel starts to extend to the north and then to the east. In the shallow area, the tunnel is narrow and "gourd-shaped." The cave starts to be filled with the oil smell from this point. The smell becomes stronger with increasing depth. Foam-like oily floats were found to be widely distributed on the water surface. In addition, there was a small amount of rubbish floating on the water. The tunnel here is not a vertical shaft; rather the underground riverbed inclines. In the "gourd-like" area, the waist width of the "gourd" is 1 m. Clay is attached to the cave wall, and the visibility of the water body is less than 50 cm. Visibility even decreases to 0 when the water becomes turbid. There was no condition for erecting the exploration guide rope in the underground river except for the upper cave wall of the "gourd." Diving work was difficult due to narrowness and low visibility. The operation was temporarily terminated after diving 15 m. The depth of this inclined tunnel was found to be about 20 m via underwater measuring instruments.
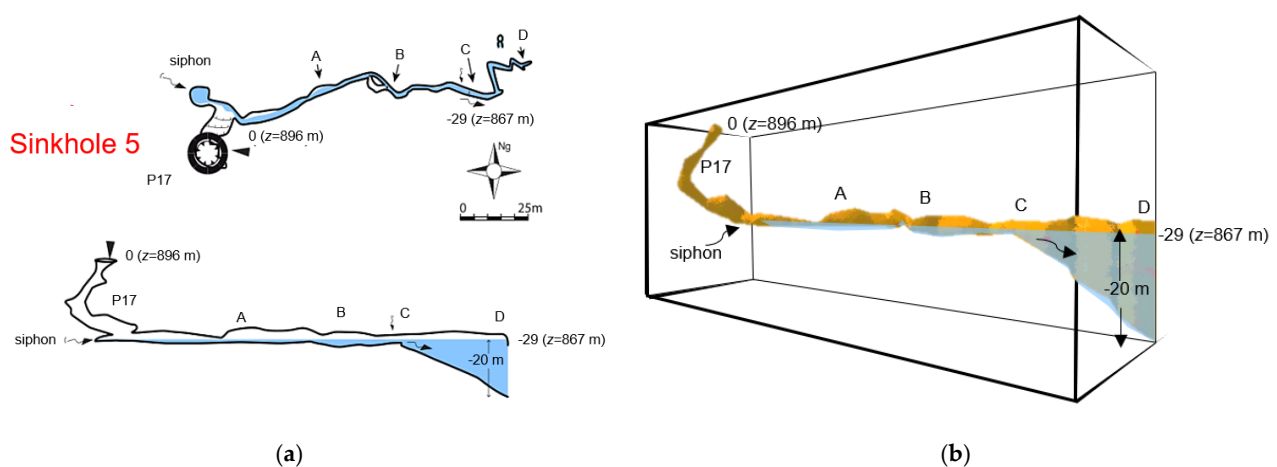

Figure 12. Sinkhole No.5: (**a**) plan; (**b**) three-dimensional layout.

The exploration in the Longdong Spring was conducted in a wave-like manner from the entrance to the right side. Gravel and soil are deposited on both sides of the cave wall.

A cave hall, including the underground river and upper cave, with an area of about 10 m^2 was detected. The outside sound could be very clearly heard from a branch above the cave hall. After continuing exploration along the water flow, it was found that the riverbed is covered with thick sediments and there is no other branch. Gravel and fine sand were found to be distributed at the bottom of the riverbed, and silt is distributed on both sides of the riverbed. Continuing diving forward, the width of the channel quickly decreases to a pathway with a width of less than 1 m and a height of 80 cm, where the water flow is relatively gentle. After that, the pathway was found to become smaller, and it became impossible to identify the compass position. For safety reasons, the diving stopped after reaching a depth of 5 m.

The measurement of flow rate at a position between Sinkhole No.5 and the Longdong Spring showed that the flow rate of the Longdong Spring is greater than that of Sinkhole No.5. Sinkhole No.5 was found to contribute about 70% of the total flow rate of the Longdong Spring; the other 30% of coal mine drainage was found to be mixed into the Longdong Spring after rainfall. Therefore, we do not need to block the unpolluted water from Sinkhole No.5.

4. Discussion

Continuous monitoring was carried out for a total of 326 times during the rainy season from May 2018 to March 2019. The flow rate and concentration of Fe in the Longdong Spring were monitored with a frequency of one time per day normally and twice per day after rainfall. The monitoring frequency returned to once per day and even once per three days when the flow rate and pollution index returned to the initial level.

4.1. Water Quality

According to preliminary investigations and water quality analysis, it was judged that the pollution is from close-range because the water quality of the spring was found to quickly improve after pollution and the polluted water was found to be similar to the drainage in the Feilong coal mine about 1 km north of the Longdong Spring. Continuous monitoring of the Longdong Spring showed that the spring water was always in a polluted state from May 2018 to 29 August 2018, as the concentration of Fe and Mn ions in the spring water were found to exceed the Standards for Drinking Water Quality (China), which states that the concentration of Fe and Mn cannot exceed 0.3 and 0.1 mg/L, respectively. After rainfall in 2017, the concentration of Fe was 33.83 mg/L; it was 62.70 mg/L in the same period in 2018, and it was as high as 94.20 mg/L on 28 June. This comparison shows that the pollution of the Longdong Spring in 2018 tended to increase during this period from May to August in the wet season.

We also found that $SO_4{}^{2-}$ and Fe are associated. In addition, the trend of the change of Mn ion was found to be roughly consistent with that of $Fe/SO_4{}^{2-}$. That is, when the concentration of $Fe/SO_4{}^{2-}$ is high, the Mn concentration is relatively high. For example, the concentration of Mn was 0.62 mg/L and the concentration of Fe was 0.3 mg/L on 23 June; the concentration of Mn and Fe increased to 20.1 and 19.1 mg/L, respectively, on 24 June.

4.2. Influence of Mine Water Level on the Spring Pollution

The goaves stopped discharging after the coal mine was abandoned in April 2017. A heavy rain on 30 June 2017 caused the pollution of the Longdong Spring. This implies that when the goaf water accumulates to such an elevation, the water overflows to the karst pathways and then mixes into the Longdong Spring. The continuous monitoring of rainfall quantity and water quality also showed that the pollution of the Longdong Spring is controlled by rainfall. Rain recharges the goaf water, and the goaf water overflows when exceeding a certain elevation. The water in the Longdong Spring became clear again and the Fe concentration was less than 0.3 mg/L at the end of August 2018 (Figure 8b) when the water level was found to reach the lowest in borehole CK-2. It can be inferred that the

water in the goaf will no longer overflow and mix with spring water when the water level in the goaf is lower than +909 m asl.

4.3. Comprehensive Analysis of Pathway with Geophysical Survey

Figure 13 shows a suspected pathway with bright gray colors from three-dimensional transient electromagnetic survey. There is an obvious pathway between the Bailachong Sinkholes group in the southwest and the Qingganglin Spring group in the southeast, which is indicated by the blue arrow. In addition, there is a suspected pathway, with a bright gray color, that is distributed from the northwest to the southeast in the northern area (red arrow 1). Here, the Dafengdong karst cave group exists, which is distributed from the southwest to northeast according to the survey. A water-conducting fractured zone near the F4 fault leads from the suspected goaves of the Feilong coal mine to the polluted Longdong Spring, extending from the northwest to southeast (red arrow 2).
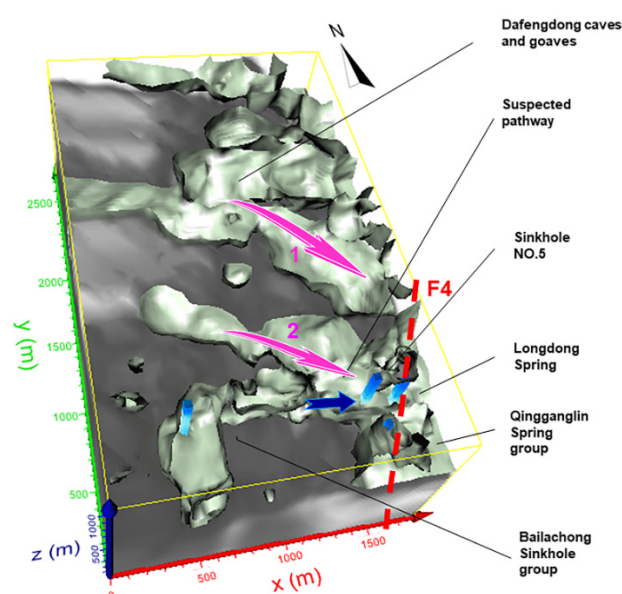

Figure 13. Suspected pathways obtained from transient electromagnetic survey.

4.4. Mechanism of the Pollution

The above-mentioned analysis shows that there is a positive correlation among the Longdong Spring water pollution, flow rate, and rainfall. When the rainfall and the flow rate are small, the spring water is not polluted, but when the rainfall and spring water flow rate in the Longdong Spring increase to certain values, the Longdong Spring becomes polluted. Secondly, the concentration of pollutants decreases due to the increased flow on the first day after heavy rain in the Longdong Spring. Third, in the dry season the pollution risk is relatively low and the flow is clear. Fourth, when the groundwater level rises to +908 m in the goaves, the spring water begins to be polluted, and when it drops below +909 m, the spring gradually reaches a stable clean state.

The pollution source of the Longdong Spring is mine water in the goaves of the Feilong coal mine, which leads to unsustainable pathway pollution under special conditions. The water above the +908 m asl in the goaf was determined as the probable source of pollution according to the geological drilling survey and results analysis. The scope of treatment can be delineated according to the analysis of hydrological and geophysical survey results. There are three suspected pathways from the south to the north: a pathway from Bailachong to Sinkhole No.5 (clear water pathway), a pathway in the southwest direction of CK-1 parallel to F4 (inferred to be a polluted pathway but not verified), and a pathway near the CK-1 borehole (a polluted pathway that has been verified as goaf) with a main direction towards the east.

5. Conclusions

Our hydrogeological investigation and survey identified the source of the pollution of the Longdong Spring. The continuous monitoring of the water quality in the Longdong Spring after April 2018 showed that the pollution of the Longdong Spring is mainly controlled by rainfall. The rainfall quantity determines the duration of pollution in the Longdong Spring. The maximum concentration of Fe and Mn in the Longdong Spring was found to exceed that in the Standard for Drinking Water Quality in China by more than 300 times. It was also concluded from hydrogeological survey that the source of pollution in the Longdong Spring is the mine water from the abandoned Feilong coal mine to the northwest. We found that the groundwater levels in the three goaves fluctuate with change in rainfall. Rainfall induces a rise in the groundwater level, which fluctuates from +908 to +914 m. It was judged that the elevation for mine water drainage to the spring in this area is approximately +908 m. Therefore, the pollution treatment range can be set at above +908 m asl.

The authors of this work ascertained the development and distribution of the pollution pathway to spring water, and they analyzed the mechanism of spring water pollution. Correlations among the Longdong Spring flow and rainfall, the groundwater level in the goaf, and spring water pollution factors show that when the mine water level in the goaf rises to +908 m after being recharged by rainfall, the pollution of spring occurs 24 h later. Two recharge pathways between the mine water and the Longdong Spring were identified. The first one is a clean groundwater pathway from the Bailachong Sinkholes to Sinkhole No.5 from the south to the north, and the second one is a polluted pathway parallel to F4 in the southwest of borehole CK-1 (judged but not verified).

Pollution control with grouting treatment is recommended to be implemented in the dry season when the flow rate of the Longdong Spring is small. The project may include grouting in the mined-out area and fan-shaped curtain grouting in the two pathways around the Longdong Spring and Sinkhole No.5, the pollution source.

Author Contributions: Conceptualization, H.R. and W.S.; methodology, H.R.; validation, W.S.; formal analysis, H.R. and W.S.; investigation, H.R.; resources, H.R.; data curation, H.R. and W.S.; writing—original draft preparation, H.R. and W.S.; writing—review and editing, W.S., X.M. and R.G.; supervision, W.S.; project administration, H.R. All authors have read and agreed to the published version of the manuscript.

Institutional Review Board Statement: Not applicable.

Informed Consent Statement: Not applicable.

Data Availability Statement: Not applicable.

References

1. Cui, Q.-L.; Wu, H.-N.; Shen, S.-L.; Xu, Y.-S.; Ye, G.-L. Chinese karst geology and measures to prevent geohazards during shield tunnelling in karst region with caves. *Nat. Hazards* **2015**, *77*, 129–152. [CrossRef]
2. Quinn, J.J.; Tomasko, D.; Kuiper, J.A. Modeling complex flow in a karst aquifer. *Sediment. Geol.* **2006**, *184*, 343–351. [CrossRef]
3. Liang, Y.; Gao, X.; Zhao, C.; Tang, C.; Shen, H.; Wang, Z.; Wang, Y. Review: Characterization, evolution, and environmental issues of karst water systems in Northern China. *Hydrogeol. J.* **2018**, *26*, 1371–1385. [CrossRef]
4. Kalhor, K.; Ghasemizadeh, R.; Rajic, L.; Alshawabkeh, A. Assessment of groundwater quality and remediation in karst aquifers: A review. *Groundw. Sustain. Dev.* **2019**, *8*, 104–121. [CrossRef]
5. Tong, L.; Fan, R.G.; Yang, S.C.; Li, C.L. Development and Status of the Treatment Technology for Acid Mine Drainage. *Min. Metall. Explor.* **2021**, *38*, 315–327.
6. Wang, X.-M. Present situation and Countermeasures of groundwater pollution in Jinci spring area. *Shanxi Water Resour.* **2000**, *3*, 14–15.
7. Zhang, J.-L. Prevention and control of groundwater pollution in closed coal mines in Zichuan District. *Ground Water* **2001**, *3*, 118–120.

8. Keqiang, H.; Yuanyuan, G.; Lu, G.; Rengang, W.; Dong, G.; Yongping, L. A systematic analysis of water flow reduction and water-quality deterioration of the Niangziguan Spring area in northern China. *Environ. Earth Sci.* **2021**, *80*, 347. [CrossRef]

9. Li., X.-D.; Cai, J.-Y.; Feng, Q.-Y.; Wang, F.-L. Experimental study on treatment of acid mine water in closed pit coal mine by dispersing alkaline matrix method. *Coal Sci. Technol.* **2020**, *48*, 160–165.

10. Gammons, C.H.; Brown, A.; Poulson, S.R.; Henderson, T.H. Using stable isotopes (S, O) of sulfate to track local contamination of the Madison karst aquifer, Montana, from abandoned coal mine drainage. *Appl. Geochem.* **2013**, *31*, 228–238. [CrossRef]

11. Kačaroğlu, F. Review of Groundwater Pollution and Protection in Karst Areas. *Water Air Soil Pollut.* **1999**, *113*, 337–356. [CrossRef]

12. Hao, Y.; Yeh, T.-C.J.; Hu, C.; Wang, Y.; Li, X. Karst groundwater management by defining protection zones based on regional geological structures and groundwater flow fields. *Environ. Geol.* **2006**, *50*, 415–422. [CrossRef]

13. Giudici, M.; Margiotta, S.; Mazzone, F.; Negri, S.; Vassena, C. Modelling hydrostratigraphy and groundwater flow of a fractured and karst aquifer in a Mediterranean basin (Salento peninsula, southeastern Italy). *Environ. Earth Sci.* **2012**, *67*, 1891–1907. [CrossRef]

14. Valdes-Abellan, J.; Pla, C.; Fernandez-Mejuto, M.; Andreu, J.M. Validating the KAGIS black-box GIS-based model in a Mediterranean karst aquifer: Case of study of Mela aquifer (SE Spain). *Hydrol. Process.* **2018**, *32*, 2584–2596. [CrossRef]

15. Jiang, C.; Gao, X.; Hou, B.; Zhang, S.; Zhang, J.; Li, C.; Wang, W. Occurrence and environmental impact of coal mine goaf water in karst areas in China. *J. Clean. Prod.* **2020**, *275*, 123813. [CrossRef]

16. Agboola, O. The role of membrane technology in acid mine water treatment: A review. *Korean J. Chem. Eng.* **2019**, *36*, 1389–1400. [CrossRef]

17. Gitari, W.M.; Petrik, L.F.; Etchebers, O.; Key, D.L.; Okujeni, C. Utilization of fly ash for treatment of coal mines wastewater: Solubility controls on major inorganic contaminants. *Fuel* **2008**, *87*, 2450–2462. [CrossRef]

18. Jin, S.; Fallgren, P.H.; Morris, J.M.; Cooper, J.S. Source Treatment of Acid Mine Drainage at a Backfilled Coal Mine Using Remote Sensing and Biogeochemistry. *Water Air Soil Pollut.* **2007**, *188*, 205–212. [CrossRef]

19. Komnitsas, K.; Bartzas, G.; Paspaliaris, I. Efficiency of limestone and red mud barriers: Laboratory column studies. *Miner. Eng.* **2004**, *17*, 183–194. [CrossRef]

20. Vymazal, J. Constructed wetlands for wastewater treatment in the Czech Republic. *Water Sci. Technol.* **2001**, *44*, 369–374. [CrossRef]

21. Li, X.-N. Study on the influence of coal mine drainage on karst water quality—Case on Shanxi Province. In Proceedings of the First National Symposium on Groundwater Development and Utilization and Pollution Control Technology Exchange, Nanjing, China, 1 June 2009; pp. 74–77.

22. Li, W.-B. Study on treatment scheme of acid mine drainage and gangue from in Yudong River Basin of Kaili City. *Heilongjiang Hydraul. Sci. Technol.* **2019**, *47*, 54–56.

23. Zhang, Z.; Xu, Y.; Zhang, Y.; Cao, J. Review: Karst springs in Shanxi, China. *Carbonates Evaporites* **2018**, *34*, 1213–1240. [CrossRef]

24. Peng, X.-C.; Wang, D. Based on groundwater pollution and prevention strategy in karst area. *Low Carbon World* **2017**, *19*, 37–38.

25. Tian, Z.-C. Key Technology of Engineering Geological Survey in Karst Area. *Value Eng.* **2020**, *39*, 186–187.

26. Available online: http://www.kaili.gov.cn (accessed on 24 August 2021).